Reprinted by: U.S. ENVIRONMENTAL PROTECTION AGENCY Add V Glaser
Office of Radiation Programs
From Radiation Data and Reports, Vol. 15, No. 4, April 1974
161-179

Microwave Hazard Measurements Near Various Aircraft Radars

[Commercial]

Richard A. Tell[1] *and John C. Nelson*[2]

In order to determine the potential for exposure of individuals when in the vicinity of aircraft radar units when aircraft are on the ground, the Electromagnetic Radiation Analysis Branch monitored four radar units that were typical of radars used by commercial aircraft. Two of the units were surveyed at a radar simulation laboratory and the other units were surveyed while in their operating positions in aircraft.

The survey determined that the radar beams from navigational and weather radar units in commercial aircraft rotate in either a sector-scanned or 360 degree rotation at approximately 15 r/min. The radar beams emanated from the aircraft above 6 feet from the ground. It was determined that power density exposures of 10 mW/cm² can occur from 8 to 18 feet from the antenna of an aircraft radar unit.

No radiation levels in excess of 0.2 mW/cm² existed in the aircraft cockpits.

This study constitutes part of a continuing effort by the Electromagnetic Radiation Analysis Branch to identify and investigate potential problem areas associated with nonionizing radiation sources in the environment. This effort was aimed at one specific class of microwave emitting equipment—aircraft radar. EPA has an interest in the possible hazards and health implications of all types of nonionizing electromagnetic sources. In this study, the principal concern developed from a desire to know the potential for exposure of individuals when in the close vicinity of aircraft radar units such as when boarding commercial air carriers. The emphasis in this study was not placed on environmental exposure at ground level resulting while aircraft are airborne but rather consists of an examination of possible thermalizing radiation levels near the radars while the aircraft are on the ground.

Data and other pertinent information relating to actual measurements were obtained during a 4-day period (4–7 September 1973) at the Federal Aviation Administration (FAA) Aeronautical Center, Oklahoma City, Okla. During this time, access was provided to a number of the FAA aircraft which are used in training exercises and routine electronic surveillance of air routes in the United States. The radar units in these planes represent a good cross section of the various aircraft radar units used in daily air passenger service in this country and represent normal complements of navigational equipment including weather and navigational radars. Additionally, access was provided to a radar simulation laboratory at which tests could be made on various radars in a test-range environment (rooftop mounted radome with adequate area to make field measurements).

Information relating to typical aircraft radar installations and radar specifications was obtained from the Electromagnetic Compatibility Analysis Center, a Department of Defense installation in Annapolis, Md. which maintains extensive computer files on radiofrequency and microwave equipment.

Objectives

The principal purposes of this study were:

1. to determine the types of radars which are used on board various commercial and private aircraft,

2. to ascertain the pertinent radar specifications which would provide an insight to the potential for hazardous exposure from these units, and

3. to make measurements of radiation levels in the vicinity of several representative radars

[1] U.S. Environmental Protection Agency, Electromagnetic Radiation Analysis Branch, Office of Radiation Programs, 9100 Brookville Road, Silver Spring, Md. 20910.

[2] Current address: Department of Physics, Midwestern University, Wichita Falls, Tex. 76308.

and compare these levels with currently accepted guidelines for safe microwave exposure.

Though the process of theoretically predicting power densities from microwave antennas is an interesting problem, this report does not contain any detailed comparisons of measured data with various analytical approaches because of the complexity of these comparisons. For more information on calculational approaches, particularly of use in the near field, the reader is directed to the appropriate references cited in the text of this report.

Typical aircraft radars

In general, large airplanes used in commercial service (e.g., DC-10, DC-9, B-727, B-707) include at least one radar and sometimes more as a part of their minimal electronic equipment. The primary radar unit normally is used for weather determination, navigation, and general search operations. These radar units are moderately powered, usually in the range of 20 to 100 kW peak power, and, as a rule, have a radar antenna which consists of a parabolic dish mounted in the very front of the aircraft. Many other radiofrequency and microwave sources are found in these aircraft, e.g., altimeters, which commonly use frequency modulated emission, pulsed sources for interrogating ground-based navigational aids such as tacan[3] units, and communications equipment. The airborne radars, however, represent the most powerful of all such equipment found aboard these vehicles and thus present the greatest potential for harmful exposure to nonaircraft personnel if care is not exercised during the operation of the equipment. A summary of radar transmitter characteristics for units found in typical airplanes in use at this time is given in table 1. This table is not intended to be exhaustive but

[3] Tacan is a condensation of tactical air navigation, a complete ultrahigh frequency polar coordinate navigation system using pulse techniques.

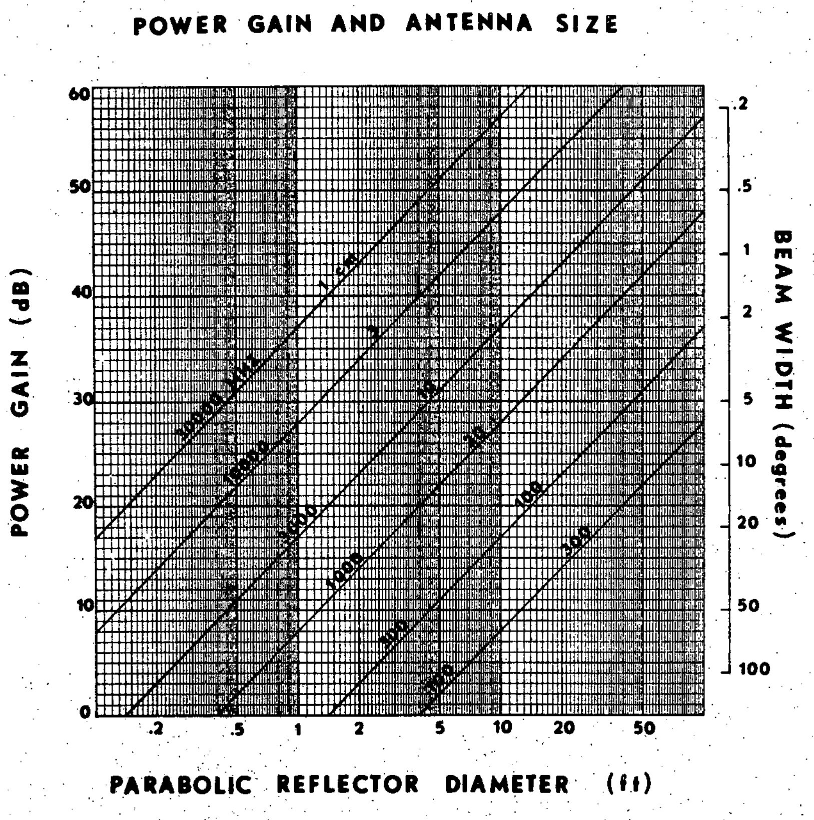

Figure 1. Relationship of dish diameter, gain, and beamwidth for selected frequencies

Table 1. Typical airborne radar specifications

Manufacturer	Model	Frequency range (MHz)	Peak power (kW)	Antenna gain (dB) [a]	Average power (W) [b]
Bendix	RDR-1A	9345-9405	17	29.5	16
	RDR-1B	9307-9405	40	31.0	25
	RDR-1B2	9345-9405	40	31.0	25
	RDR-1C	5370-5430	100	30.0	80
	RDR-1D	9345-9405	17	29.5	16
	RDR-1E	9345-9405	65	37.1	65
	RDR-1F	9300-9500	65	31.0	80
RCA	AVQ-10	5380-5420	75	28.0	60
	AVQ-20	9335-9415	20	27.5	16
	AVQ-30C	5370-5430	60	30.0	122
	AVQ-30X	9315-9375	60	26.0	69
Collins	WP-101	5370-5430	75	33.0	66

[a] The antenna gains listed here are those for a parabolic antenna dish in a typical radar configuration. Manufacturers normally offer more than one size dish for their transmitter, and thus the gain may vary slightly from one installation to another.

[b] The average power from any particular radar system may have several different values depending on the exact pulse width and pulse repetition frequency (PRF) selected. This column lists the highest of the average powers if more than one is possible.

rather indicative of the specifications of typical airborne radars used aboard large aircraft.

As noted in the table, the antenna gain may vary, depending on the actual antenna size employed. The gain of a parabolic dish is a function of its diameter. Figure 1 illustrates the relationship between dish diameter, gain, and beamwidth for several different frequencies. Gain of a well-designed horn-fed parabolic reflector may be estimated from the relationship (*1*):

$$G = 27\,000/(\theta_H \cdot \theta_E)$$

where:

G = absolute gain above an isotropic radiator,

θ_H = 3 dB beamwidth (in degrees) in the H plane of the antenna,

θ_E = 3 dB beamwidth (in degrees) in the E plane of the antenna.

Radar antenna patterns may be shaped differently. The two most commonly used shapes are a narrow "pencil" beam in which the beam is made as narrow as the dish allows, and a cosecant-squared shape applied to the vertical pattern. A cosecant-squared shape refers to the proportionality in the vertical plane of antenna gain to the cosecant squared of the elevation angle. Such a vertical pattern in practical antennas varies as cosecant squared from about the upper 3 dB point to approximately 40 degrees in elevation. Using a vertical cosecant squared radiation pattern allows constant power density illumination of a target as long as the target maintains a constant altitude.

For purposes of estimating the radiation exposure level from a radar, it is necessary, as a minimum, to know the effective radiated power (ERP) from the antenna. This ERP is a measure of the antenna's focusing power and is equal to the product of antenna input power and antenna gain. At distances on the order of $2D^2/\lambda$ or greater (D is the largest dimension of the antenna, the diagonal for rectangular units, and λ is the free space wavelength of the transmitted wave). The power density (for hazard purposes) may be computed from:

$$W = \frac{PG}{4\pi R^2}$$

where,

W = power density at a distance R from the antenna,

P = power available to antenna (taking into account transmission lone losses), and

G = absolute mainbeam gain of the antenna.

This equation is valid only for points on the axis of the mainbeam of the antenna and at distances which are in the far field. For computations of power density at points within the near field, more complicated techniques are required—in this case, the antenna gain must be corrected for application at near field distances. Though exact formulas are difficult to arrive at, the Army has developed some simple equations for use in the near field of circular parabolic antennas on the basis of empirical data (*2*). Other discussions of near field corrections may be found in the literature (*3,4*).

The power densities computed from any of the equations will be peak or average values depending on the power term entered in the equation. Currently, for hazard purposes, the average power to the antenna is taken as the power which is proportional to the tissue heating effectiveness of the radiation exposure. Peak power densities, especially from pulsed sources such as radars, may be important in various device interferences (*5*). For practical purposes in radar computations, in lieu of actual power measurements, the average power of a transmitter (P_{avg}) is taken as

$$P_{avg} = P_{peak} \cdot PRF \cdot \tau$$

where:

P_{peak} = the peak pulse power (in watts) of the radar transmitter (this is almost always the stated power of radar),

PRF = the pulse repetition frequency (hertz),

τ = the pulse width (seconds).

Figure 2 plots the relation between peak and average power for various PRF's and pulse widths.

Radars and facilities available for test

This section describes the radar units which were surveyed and circumstances under which the measurements were made. It was the intent of the authors to obtain measurement data on several different, but typical, radar types in common use. Under the constraints of the time available, the poor weather conditions, and other measurement projects being conducted during the trip, a total of four radars were surveyed which represent three different models and manufacturers. Prior to making measurements around the radar units mounted in the airplane nose cones, a series of measurements were obtained on similar radars at the radar simulation laboratory. At the simulation facility, actual radars could be operated at will in a relatively controlled environment. Figure 3 depicts the interior of the simulation lab, show-

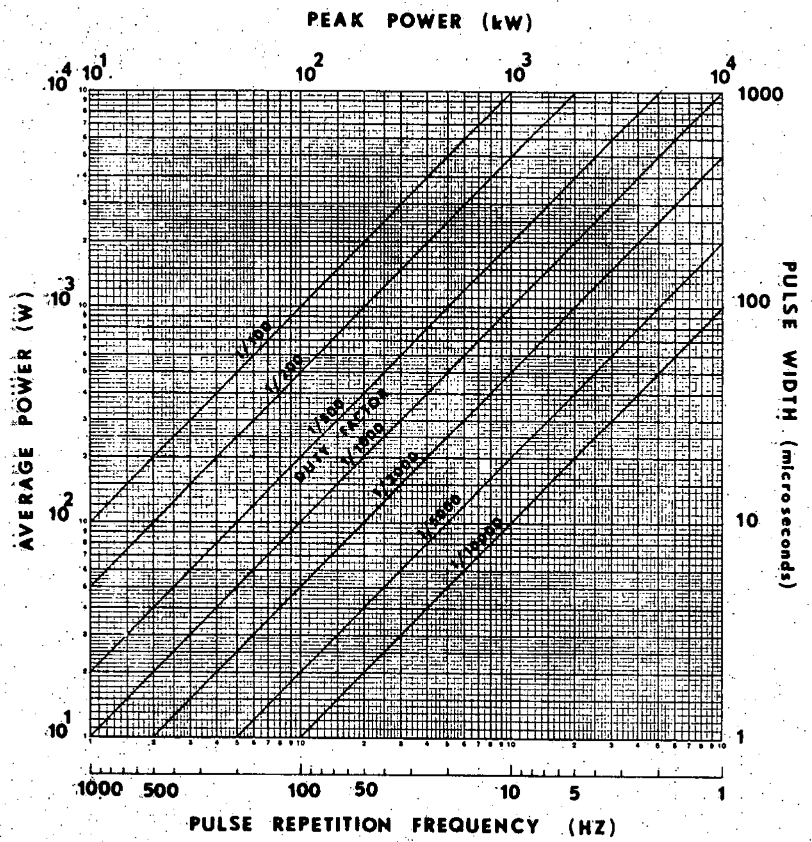

Figure 2. Relationship of peak and average power

Figure 3. Interior of simulation laboratory

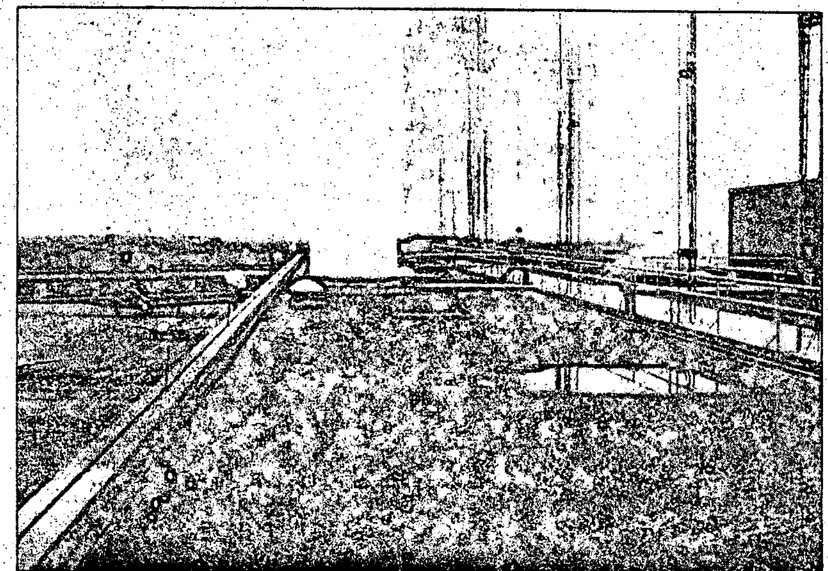

Figure 4. Roof-mounted radome

ing the various power supplies, test equipment, and radar control panels. The actual transmitter unit and antenna were placed on a platform which could be elevated into a radome structure on the roof above the laboratory (figure 4). Notice the large number of communication antennas in the near vicinity. A closeup view of a typical airborne radar dish antenna is shown in figure 5.

Table 2 lists the radars which were measured and their installation configurations. Detailed specifications for each of these radars may be found in tables 3, 4, and 5. The Bendix RDR-1B is capable of two different pulse widths and these are indicated in the table. Also given in these tables are the calculated values for $2D^2/\lambda$, the far-field distance as computed from reference (*2*) ($D^2/2.83\lambda$), the maximum power density expected in the near-field region based on reference (*3*), and the distance to the point where the field is expected to be 10 mW/cm^2, assuming a far-field gain for the specific antenna. The gain of an antenna is always a far-field gain unless otherwise stated (i.e., the gain of an antenna is always that gain which is effective at a distance where the power density decreases as inverse square distance).

Table 2. Summary of radars used in measurements

Radar	Manufacturer	Simulation laboratory	Aircraft
AVQ-10	RCA	X	X
RDR-1B	Bendix	X	
WP-103	Collins		X

The two aircraft radar units surveyed were both installed in the nose cones of their respective planes—a Sabre Liner with the Collins WP-103 and a Convair 600 with the RCA AVQ-10. Figures 6 and 7 show these aircraft parked in the flight operations area of the FAA

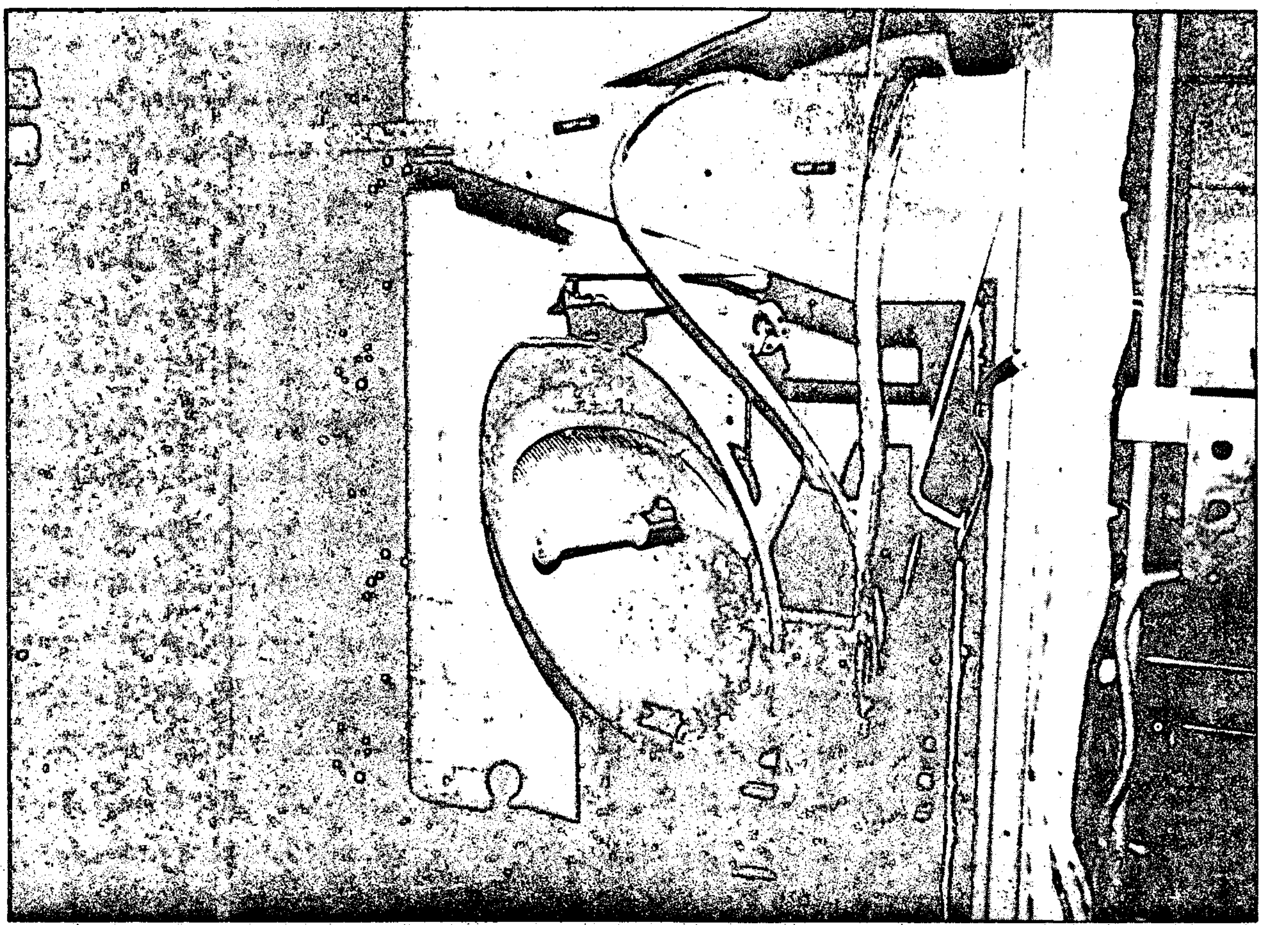

Figure 5. Typical airborne radar dish

Table 3. Specifications for RCA AVQ-10 aircraft radar

Antenna diameter	22 inches	
Transmitting frequency	5400±20 MHz	
Wavelength	5.55 cm	
Pulse width	2 μs	
Pulse repetition frequency	400 Hz	
Duty factor	0.0008	
1/duty factor	1250	
Peak power output	75 kW	
Average power output	60 W	
Antenna gain	33 dB	
Maximum average effective radiated power	120 kW	
Antenna scan angle	360°	
Antenna tilt limits	10° up – 15° down	
Antenna rotation speed	15 r/min	
3 dB beam width:	Horizontal	Vertical
Pencil beam	4.5°	4.5°
CSC^2 beam	4.5°	(a)
Polarization:		
Pencil beam	Horizontal	
CSC^2 beam	(a)	
Calculated data:		
$2D^2/\lambda$	11 m (36 feet)	
Distance to beginning of far field ($D^2/2.83\lambda$)	2.0 m (6.6 feet)	
Maximum peak power density in near field	120 W/cm^2	
Maximum average power density in near field	100 mW/cm^2	
Distance to 10 mW/cm^2 assuming far field gain	10 m (33 feet)	

a Information not available.

Table 4. Specifications for Bendix RDR-1B aircraft radar

Antenna diameter	22 inches	
Transmitting frequency	9375±30 MHz	
Wavelength	3.20 cm	
Pulse width	1.5 μs search; 2.25 μs beacon	
Pulse repetition frequency	400 Hz	
Duty factor	0.0006; 0.0009	
1/duty factor	1667; 1111	
Peak power output	40 kW	
Average power output	24 W; 36 W	
Antenna gain	30.0 dB	
Maximum average effective radiated power	24 kW; 36 kW	
Antenna scan angle	360°	
Antenna tilt limits	15° up – 15° down	
Antenna rotation speed	15 ± 3 r/min	
3 dB beam width:	Horizontal	Vertical
Pencil beam	3.8°	3.8°
CSC^2 beam	3.8°	(a)
Polarization:		
Pencil beam	Horizontal	
CSC^2 beam	Vertical	
Calculated data:		
$2D^2/\lambda$	20 m (66 feet)	
Distance to beginning of far field ($D^2/2.83\lambda$)	3.5 m (11 feet)	
Maximum peak power density in near field	65 W/cm^2	
Maximum average power density in near field	39 mW/cm^2 (at 24 kW ERP); 59 mW/cm^2 (at 36 kW ERP)	
Distance to 10 mW/cm^2 assuming far field gain	4.4 m (14 feet) (at 24 kW ERP); 5.4 m (18 feet) (at 36 kW ERP)	

a Information not available.

center. Careful examination of figure 7 reveals the nearby control towers and weather radar at Will Rogers Airport.

Survey equipment

All measurements of radiation levels covered by this report were made with a Narda Microwave Corporation Model 8300 broadband isotropic radiation monitor. This monitor consisted of a Model 8321 isotropic probe (rated for a maximum time average power density of 20 mW/cm^2 for pulsed fields), and a Model 8310 probe readout meter. Salient characteristics of this device are given in table 6. This particular device, Serial Number 02006, was certified as being calibrated 18 June 1973, or approximately 2.5 months prior to the field trip.

Table 5. Specifications for Collins WP-103 aircraft radar

Antenna diameter	12 inches	
Transmitting frequency	9375±40 MHz	
Wavelength	3.20 cm	
Pulse width	2.3 μs nominal	
Pulse repetition frequency	400 Hz	
Duty factor	0.0008–0.001	
1/Duty factor	1000 (assuming 0.001 DF)	
Peak power output	20 kW	
Average power output	20 W (assuming 0.001 DF)	
Antenna gain	26 dB	
Maximum average effective radiated power	8 kW	
Antenna scan angle	120° sector	
Antenna tilt limits	12° up–12° down	
Antenna rotation speed	15 r/min	
3 dB beam width:	Horizontal	Vertical
Pencil beam	(a)	(a)
CSC² beam	(a)	(a)
Polarization:		
Pencil beam	Horizontal	
CSC² beam	(a)	
Calculated data:		
2 D²/λ	5.8 m (19 feet)	
Distance to beginning of far field (D²/2.83λ)	1.0 m (3.4 feet)	
Maximum peak power density in near field	110 W/cm²	
Maximum average power density in near field	110 mW/cm²	
Distance to 10 mW/cm² assuming far field Gain	2.5 m (8.3 feet)	

a Information not available.

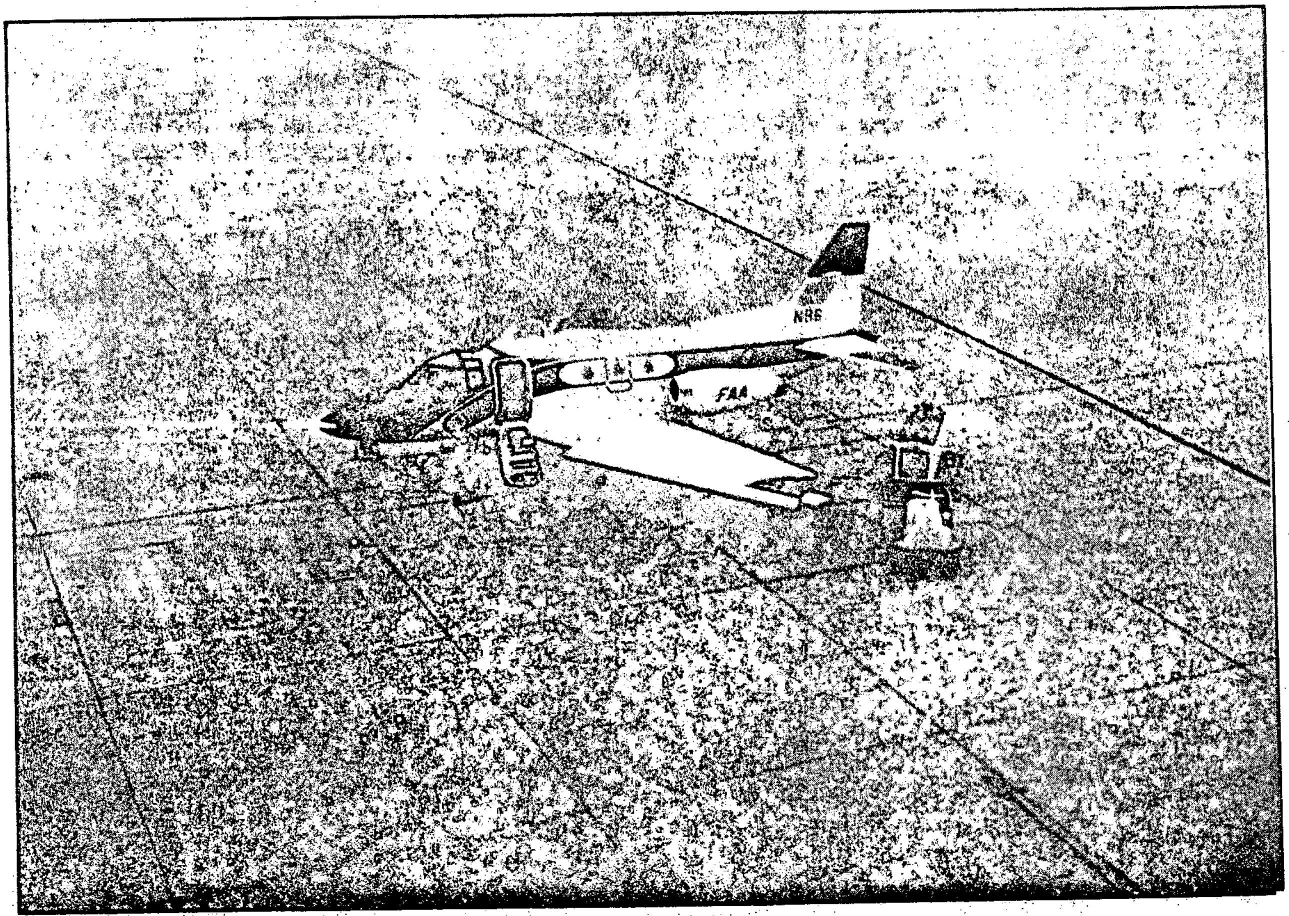

Figure 6. Sabre Liner

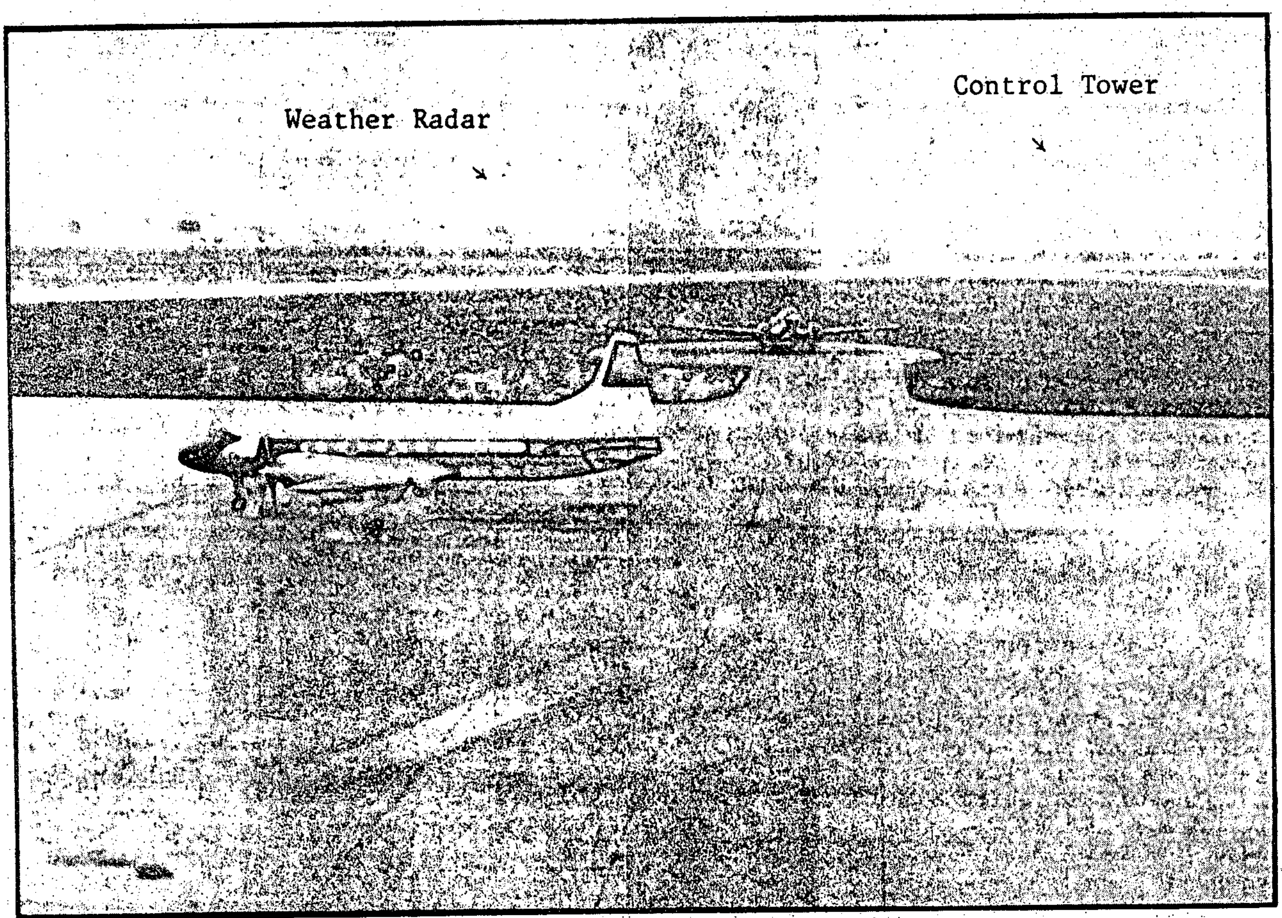

Figure 7. Convair 600

Table 6. Characteristics of a Narda Microwave Corporation Model 8300 broad band isotropic radiation monitor

Frequency range	0.3 to 18 GHz
Power reading ranges	Full scale (two ranges) 2 mW/cm^2 and 20 mW/cm^2
Accuracy of isotropic probe calibration	±0.5 dB
Isotropic probe time constant	20 ms
Frequency sensitivity from 1 to 12 GHz from 0.85 to 16 GHz from 0.30 to 18 GHz	 ±0.5 dB +0.5, −1 dB +0.5, −3 dB
Isotropic response	±0.5 dB maximum deviation from energy incident in any direction except from and through handle
Response time, including time for meter indicator to to reach 90% of final steady state reading when subjected to a stepped input signal	1.2 s
Accuracy of instrumentation	±3% of full scale
Probe overload rating Continuous wave (cw) Peak (pulsed emissions)	 100 mW/cm^2 20 W/cm^2

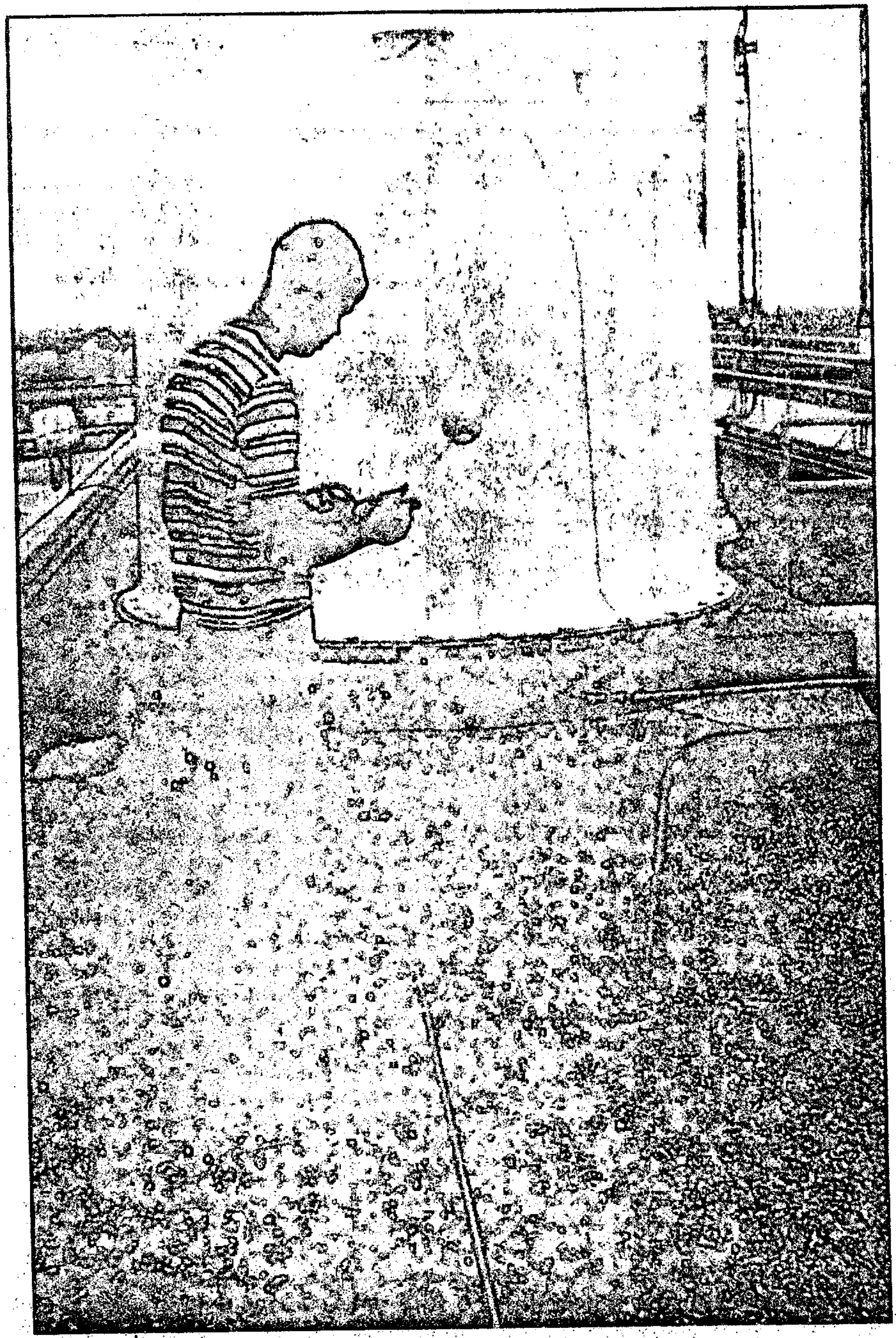

Figure 8. Roof radome survey

Procedures

At the simulation lab, each of the two radars was individually set up so that the radar dish could be elevated to the roof-mounted radome where field measurements were obtained by standing on the flat portion of the roof in the vicinity of the radome. In this manner, a relatively free field situation prevailed, tending to minimize reflection problems. All data were collected with the radar dishes stopped in azimuthal rotation; this was necessary (a) to ensure that all readings were being taken in the main radiation lobe of the transmitting dish, and (b) to obtain true readings of maximum levels because the time response of the indicator circuitry was slow. Once the dish was aligned as desired, the RF power was applied, and field measurements were made approaching the radome from a distance of approximately 100 feet. Once a rough feel for the magnitude of the fields was obtained, careful measurements were then made at successively shorter distances to the radome. All such measurements were obtained by holding the isotropic probe in one hand, the metering device in the other hand, and searching for the mainbeam of the dish at each distance. Distances were measured with a 100-foot steel tape laid on the roof. As one individual made the measurements, another recorded the data (field level and distance) at a lateral distance sufficient to not cause noticeable field reflections toward the survey probe. Data was taken in this manner until a distance was reached where the peak power density was equal to the burn-out limit for the survey instrumentation (20 W/cm²). This peak field value was predetermined in terms of the meter indication of time average power density by taking into account the duty factor of each radar. In practical terms, this imposed a limit in the neighborhood of 15–18 mW/cm² average power density for the radars tested.

Figure 8 shows a typical survey reading being taken near the radome. After conducting the mainbeam field measurements for each radar, a survey of the area immediately adjacent to the radome was made, completely encircling the radome except for the mainbeam area in front of the antenna. These measurements were made to determine the possible existence of side lobes and a back lobe for the antenna. Figure 9 shows a measurement being made inside the radome but to the rear of the transmitting dish. In all cases, inadvertent exposure to individuals, other than the authors, was prevented by keeping other personnel off the roof.

A similar approach was used with those radars actually in an airplane. The planes were parked in open areas, clear of obstructions, adjacent to taxiways in accordance with FAA advice (*6*). Measurements were never taken with an airplane parked inside of a hangar. Under such conditions, reflections from other nearby aircraft could cause radar receiver crystal damage. Accordingly, when weather

Figure 9. Measurement inside radome

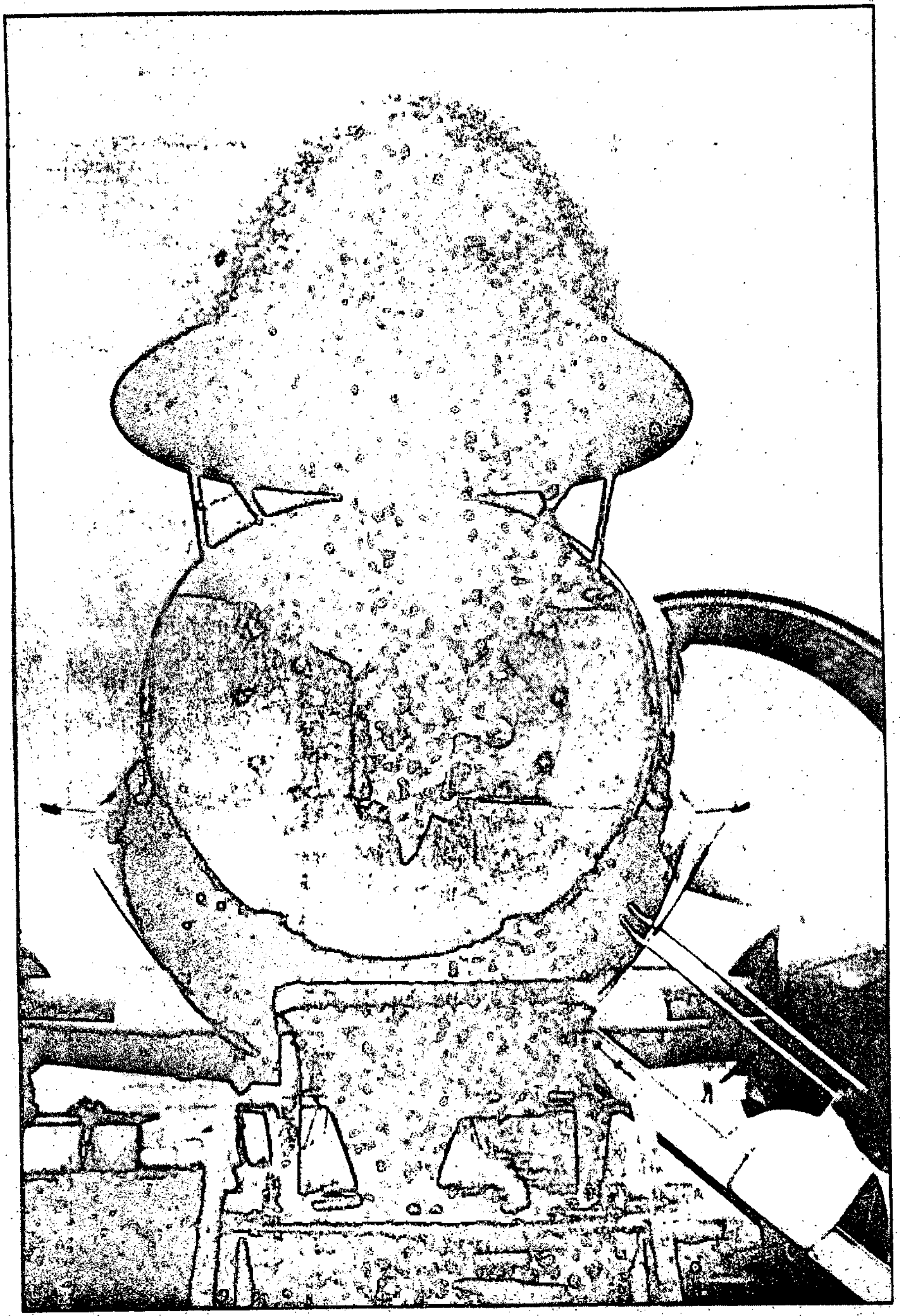

Figure 10. Convair with nose cone lifted

permitted, the selected airplane was moved to the outside location and the antenna fixed in position, pointing straight ahead of the plane. With the Convair 600 (figure 10) the nose cone was lifted on its hinge and measurements made as a function of distance, approaching the nose from a distance. Figure 11 is another picture of the survey of the Convair. Because of the height of the Convair nose above ground, the dish had to be pointed downward at approximately a 13° tilt in order that field measurements could be made from the ground. With

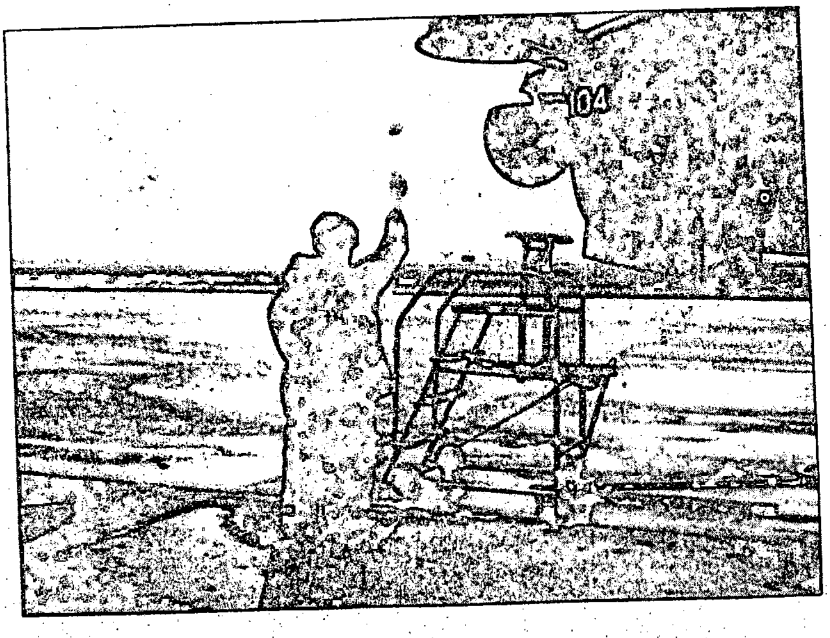

Figure 11. Survey of Convair

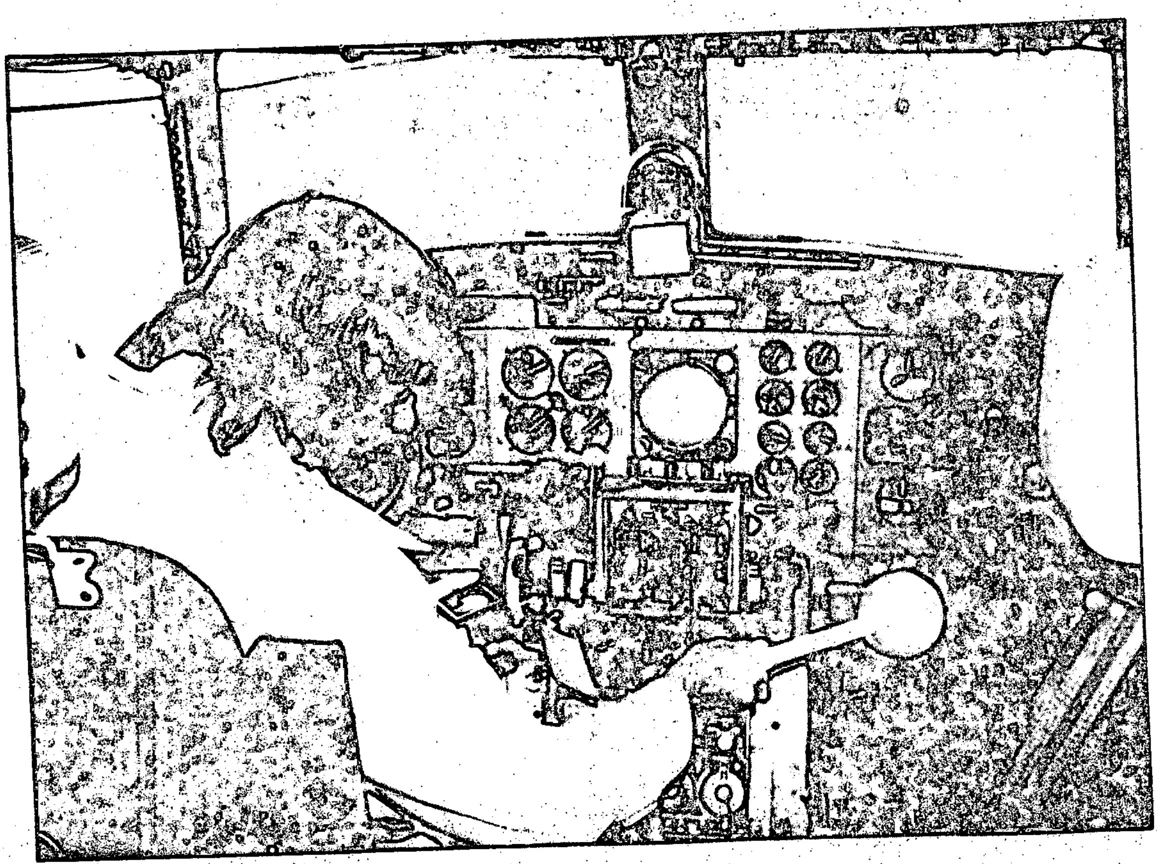

Figure 12. Survey of Convair cockpit

such an orientation, ground reflections were observed from the concrete apron at certain distances.

Once measurements on the dish axis were completed on the Convair, the antenna was repositioned until it pointed directly toward the cockpit, so that a survey of the cockpit could be made for possible radiation exposure (figure 12). The antenna was then positioned at various angles to enhance possible reflection from wings and other aircraft structures while additional cockpit measurements were made. Notice that the front of the fuselage is a flat metal plate which effectively shields the cockpit from the dish. This plate is covered with an absorptive, anechoic material to prevent receiver failure during the time that the antenna is rotating to the rear, since full 360 degree rotation is used by the AVQ-10.

Finally, a measurement was made of the attenuation properties of the nose cone itself, since our measurements were unattenuated ones. This was accomplished by lowering the nose cone, determining the radiation intensity at a known distance, and comparing with previous unattenuated values at the same distance.

Measurements on the WP-103 in the Sabre Liner were simplified in that the plane is smaller and consequently lower to the ground. This factor allowed the antenna to be kept nearly perfectly horizontal, and thus fewer ground reflection problems were observed. Also, due to the inconvenience of the operation, the nose cone itself was not removed. Instead, a portion of the fuselage shell near the nose cone was removed, so that adjustments could be made for stopping the normal antenna rotation. Figure 13 shows surveying around the Sabre Liner.

Results

The field intensity data resulting from our measurements are plotted in figures 14, 15, and 16. Survey data for the simulation lab measurements on a Bendix RDR-1B and the RCA AVQ-10 are shown in figure 14. Actual data points are graphed and a smooth curve was visually fitted through these points. Also shown on each graph is the distance at which the far field begins, as calculated by reference (2) and indicated under calculated data in tables 3, 4, and 5.

At various distances, more than one power density value was obtained. Such occurrences could be due to (a) practical difficulties encountered in relocating the same exact measurement position with respect to the main beam, and (b) apparent power fluctuations in the RF output from the radar transmitter. This was

Figure 13. Survey around Sabre Liner

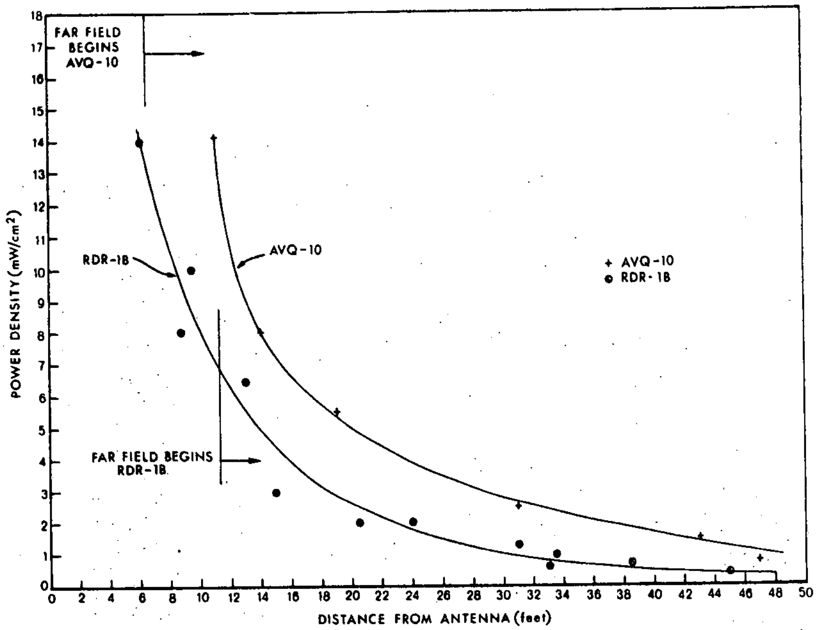

Figure 14. Measurements at simulation lab with radome

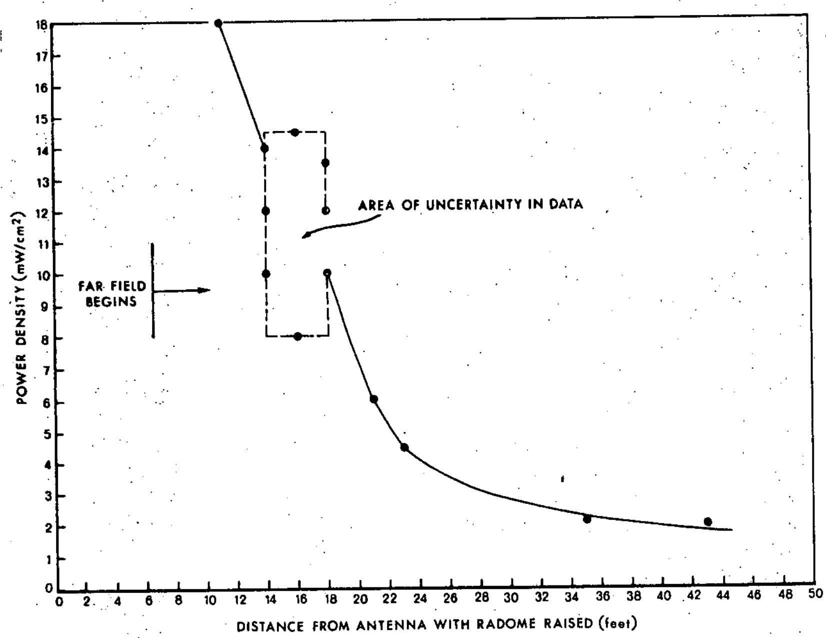

Figure 15. Measurements of RCA AVQ–10 in Convair 600

most evident in measurements on the RDR-1B and the Convair installation of the AVQ-10. In particular, stationary monitoring at a given distance would, from time to time, produce a variation in the power density reading, indicating some transmitter instability. However, notice that the area of data scatter in the RDR-1B measurements falls within the near field range and consequently is possibly an indication of the very erratic nature of this particular region of the exposure field, causing extreme difficulty in repositioning the probe to the same exact point, on a repetitive basis. Table 7 summarizes the data, indicating the distance at which the exposure power density was found to be 10 mW/cm² and 1 mW/cm²

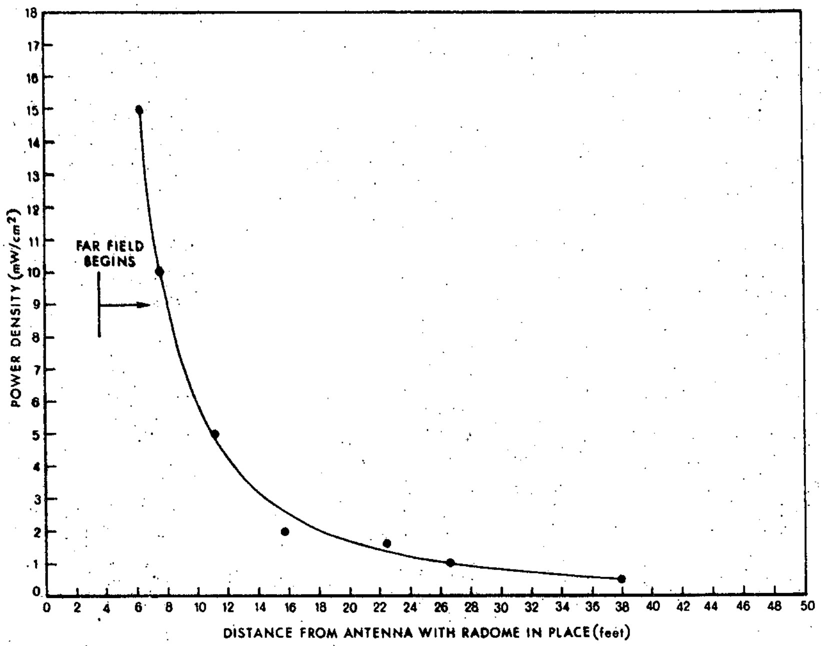

Figure 16. Measurements of Collins WP–103 in Sabre Liner

Table 7. Summary of exposures from radars

Radar configuration	Approximate distance (feet) to exposure of:	
	10 mW/cm²	1 mW/cm²
RDR–1B (simulation lab)	9	34
AVQ–10 (simulation lab)	12	47
AVQ–10 (Convair)	18	50+
WP–103 (Sabre Liner)	8	27

for each of the respective radar configurations. From the data, it appears that exposures in the neighborhood of 10 mW/cm² may occur in the general range of 8 to 18 feet from the antenna, dependent on the particular radar and conditions under which it might be measured (ground reflections included, radome losses, etc.).

Measurement of the Convair 600 nose cone radome showed an attenuation of approximately 5.5 dB or a power reduction factor of 0.28.

When measurements were made about the perimeter of the simulation lab radome, no detectable radiation lobes were apparent at the 0.2 mW/cm² level for either the RDR-1B or the AVQ-10. When approaching the transmitting dish at extremely close-in distances inside the radome, some low-level fields were observed at about 2 feet from the side of the dish.

A survey of the cockpit area of both the Sabre Liner and Convair 600 also showed that no detectable radiation at the 0.2 mW/cm² level was present (0.2 mW/cm² is the minimum detection capability of the Narda instrument). This was not surprising in the case of the Convair since a good shielding effect was produced by the fuselage shell between the cockpit and the radar antenna. With the Convair, the worst possible antenna position was used for these measurements—it was positioned directly toward the cockpit. Other directions were tried to see if reflections might occur from the wing or propeller structures on the aircraft causing scattering into the cockpit. Again, nothing detectable was observed in the cockpit (including ground reflection, radome losses, etc). However, when the probe was held at arm's length out of the pilot's window (left-hand side) some minimal upscale reading was observed (something slightly greater than 0.2 mW/cm²).

In similar measurements on the Sabre Liner, no detectable levels were found in the cockpit.

In this case, however, the radar dish is sector scanned and limited to principally the front 270° of view.

Conclusions

On the basis of this study, the following conclusions have been reached:

a. Typical maximum power for aircraft radars lies in the range 20 to 100 kW peak and 20 to 120 W average power.

b. Antenna gains are normally in the range of 25 to 30 dB.

c. Peak ERP is in the range of 6 MW to 100 MW while average ERP is in the range of 6 kW to 120 kW.

d. Exposures to power densities of 10 mW/cm^2 can occur in the range of 8 to 18 feet from the antenna.

e. Aircraft radomes can exhibit attenuations of about 5.5 dB.

f. No radiation levels in excess of 0.2 mW/cm^2 existed in the aircraft cockpits.

g. Normally, airborne radar antennas are rotating devices with either sector scanned or full 360 degree rotation at approximately 15 r/min.

h. In general, the radar beams on commercial aircraft are above 6 feet in height from the ground.

i. Reliable survey data can be obtained only by stopping the antenna rotation.

j. Reflections from nearby objects, including the ground, tend to cause irregularities in the field structure. Because of the unknown phase characteristics of the reflected waves, actual measurements are preferable to determine exposure in these situations.

k. Use of far field antenna gain was not reliable for predicting distances to the 10 mW/cm^2 exposure level.

Recommendations

Further investigation with respect to this study which could add useful information to the question of human exposure from airborne radar would be a determination of possible passenger exposure distances which can be found at airports. This information would prove interesting from the standpoint of an inadvertent exposure occurring when the airplane is parked near areas with passenger waiting rooms. Under such circumstances and depending upon the exact plane-waiting room configuration, potential short-burst radiation levels could be reasonably high. Assuming an instantaneous time average exposure of 5 mW/cm^2, the peak power density could be about 5 W/cm^2.

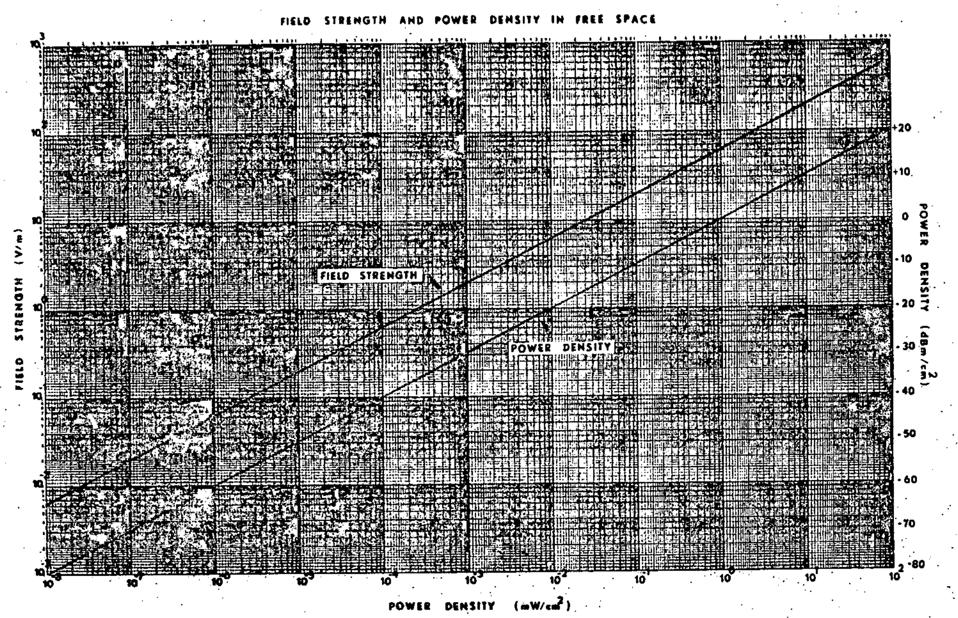

APPENDIX A. Field strength and power density in free space

VOLTAGE RATIO	POWER RATIO	dB	VOLTAGE RATIO	POWER RATIO	VOLTAGE RATIO	POWER RATIO	dB	VOLTAGE RATIO	POWER RATIO
1.0000	1.0000	0.00	1.0000	1.0000	.5129	.2630	5.8	1.950	3.802
.9988	.9977	0.01	1.0012	1.0023	.5070	.2570	5.9	1.972	3.890
.9977	.9954	0.02	1.0023	1.0046	.5012	.2512	6.0	1.995	3.931
.9966	.9931	0.03	1.0035	1.0069	.4955	.2455	6.1	2.018	4.074
.9954	.9908	0.04	1.0046	1.0093	.4898	.2399	6.2	2.042	4.169
.9943	.9886	0.05	1.0058	1.0116	.4842	.2344	6.3	2.065	4.266
.9931	.9863	0.06	1.0069	1.0139	.4786	.2291	6.4	2.089	4.365
.9920	.9840	0.07	1.0081	1.0162	.4732	.2239	6.5	2.113	4.467
.9908	.9817	0.08	1.0093	1.0186	.4677	.2188	6.6	2.138	4.571
.9897	.9795	0.09	1.0104	1.0209	.4624	.2138	6.7	2.163	4.677
.9886	.9772	0.1	1.012	1.023	.4571	.2089	6.8	2.188	4.786
.9772	.9550	0.2	1.023	1.047	.4519	.2042	6.9	2.213	4.898
.9661	.9333	0.3	1.035	1.072	.4467	.1995	7.0	2.239	5.012
.9550	.9120	0.4	1.047	1.096	.4416	.1950	7.1	2.265	5.129
.9441	.8913	0.5	1.059	1.122	.4365	.1905	7.2	2.291	5.248
.9333	.8710	0.6	1.072	1.148	.4315	.1862	7.3	2.317	5.370
.9226	.8511	0.7	1.084	1.175	.4266	.1820	7.4	2.344	5.495
.9120	.8318	0.8	1.096	1.202	.4217	.1778	7.5	2.371	5.623
.9016	.8128	0.9	1.109	1.230	.4169	.1738	7.6	2.399	5.754
.8913	.7943	1.0	1.122	1.259	.4121	.1698	7.7	2.427	5.888
.8810	.7762	1.1	1.135	1.288	.4074	.1660	7.8	2.455	6.026
.8710	.7586	1.2	1.148	1.318	.4027	.1622	7.9	2.483	6.166
.8610	.7413	1.3	1.161	1.349	.3981	.1585	8.0	2.512	6.310
.8511	.7244	1.4	1.175	1.380	.3936	.1549	8.1	2.541	6.457
.8414	.7079	1.5	1.189	1.413	.3890	.1514	8.2	2.570	6.607
.8318	.6918	1.6	1.202	1.445	.3846	.1479	8.3	2.600	6.761
.8222	.6761	1.7	1.216	1.479	.3802	.1445	8.4	2.630	6.918
.8128	.6607	1.8	1.230	1.514	.3758	.1413	8.5	2.661	7.079
.8035	.6457	1.9	1.245	1.549	.3715	.1380	8.6	2.692	7.244
.7943	.6310	2.0	1.259	1.585	.3673	.1349	8.7	2.723	7.413
.7852	.6166	2.1	1.274	1.622	.3631	.1318	8.8	2.754	7.586
.7762	.6026	2.2	1.288	1.660	.3589	.1288	8.9	2.786	7.762
.7674	.5888	2.3	1.303	1.698	.3548	.1259	9.0	2.818	7.943
.7586	.5754	2.4	1.318	1.738	.3508	.1230	9.1	2.851	8.128
.7499	.5623	2.5	1.334	1.778	.3467	.1202	9.2	2.884	8.318
.7413	.5495	2.6	1.349	1.820	.3428	.1175	9.3	2.917	8.511
.7328	.5370	2.7	1.365	1.862	.3388	.1148	9.4	2.951	8.710
.7244	.5248	2.8	1.380	1.905	.3350	.1122	9.5	2.985	8.913
.7161	.5129	2.9	1.396	1.950	.3311	.1096	9.6	3.020	9.120
.7079	.5012	3.0	1.413	1.995	.3273	.1072	9.7	3.055	9.333
.6998	.4898	3.1	1.429	2.042	.3236	.1047	9.8	3.090	9.550
.6918	.4786	3.2	1.445	2.089	.3199	.1023	9.9	3.126	9.772
.6839	.4677	3.3	1.462	2.138	.3162	.1000	10.0	3.162	10.000
.6761	.4571	3.4	1.479	2.188	.2985	.08913	10.5	3.350	11.22
.6683	.4467	3.5	1.496	2.239	.2818	.07943	11.0	3.548	12.59
.6607	.4365	3.6	1.514	2.291	.2661	.07079	11.5	3.758	14.13
.6531	.4266	3.7	1.531	2.344	.2512	.06310	12.0	3.981	15.85
.6457	.4169	3.8	1.549	2.399	.2371	.05623	12.5	4.217	17.78
.6383	.4074	3.9	1.567	2.455	.2239	.05012	13.0	4.467	19.95
.6310	.3981	4.0	1.585	2.512	.2113	.04467	13.5	4.732	22.39
.6237	.3890	4.1	1.603	2.570	.1995	.03981	14.0	5.012	25.12
.6166	.3802	4.2	1.622	2.630	.1884	.03548	14.5	5.309	28.18
.6095	.3715	4.3	1.641	2.692	.1778	.03162	15.0	5.623	31.62
.6026	.3631	4.4	1.660	2.754	.1585	.02512	16.0	6.310	39.81
.5957	.3548	4.5	1.679	2.818	.1413	.01995	17.0	7.079	50.12
.5888	.3467	4.6	1.698	2.884	.1259	.01585	18.0	7.943	63.10
.5821	.3388	4.7	1.718	2.951	.1122	.01259	19.0	8.913	79.43
.5754	.3311	4.8	1.738	3.020	.1000	.01000	20.0	10.000	100.00
.5689	.3236	4.9	1.758	3.090	.03162	.00100	30.0	31.620	1,000.00
.5623	.3162	5.0	1.778	3.162	.01	.00010	40.0	100.00	10,000.00
.5559	.3090	5.1	1.799	3.236	.003162	.00001	50.0	316.20	10^5
.5495	.3020	5.2	1.820	3.311	.001	10^{-6}	60.0	1,000.00	10^6
.5433	.2951	5.3	1.841	3.388	.0003162	10^{-7}	70.0	3,162.00	10^7
.5370	.2884	5.4	1.862	3.467	.0001	10^{-8}	80.0	10,000.00	10^8
.5309	.2818	5.5	1.884	3.548	.00003162	10^{-9}	90.0	31,620.00	10^9
.5248	.2754	5.6	1.905	3.631	10^{-5}	10^{-10}	100.0	10^5	10^{10}
.5188	.2692	5.7	1.928	3.715					

Figure 15. APPENDIX B. Voltage and power ratios to dB

Acknowledgements

The authors are especially grateful to the FAA staff who assisted in this field trip: Dr. Robert N. Thompson and Mr. Jim D. Langwell of the Industrial Hygiene Section in the Civil Aeromedical Institute for their excellent cooperation and coordination of facilities and personnel involved in this measurement study; Mr. Harold K. Harvell, Chief of the Aircraft and Avionics Maintenance Branch, Aircraft Services Base, for his help in making arrangements for access to aircraft and the radar simulation lab; Mr. Alvin E. Kounovsky and Mr. George F. Bonner in the Avionics Maintenance Section, for their instruction and assistance in the operation of laboratory radar equipment; Mr. Jim L. McCloskey and Mr. John E. Burleson in the Avionics Maintenance Section for their patience and assistance in setup and operation of radars mounted in the airplanes.

REFERENCES

(*1*) Reference Data for Radio Engineers. Howard W. Sams and Co., Indianapolis, Ind. (1972) pp. 29-32.

(*2*) PALMISANO, W. A. and D. H. SLINEY, Instrumentation and methods used in microwave hazard analysis. Presented at the American Industrial Hygiene Association Meeting, Chicago, Ill. (4 May 1967).

(*3*) MUMFORD, W. W. Some technical aspects of microwave radiation hazards. Proceedings of the IRE (February 1961) pp. 427-447.

(*4*) U.S. AIR FORCE. Electromagnetic radiation hazards, Technical Manual T.O. 31Z-10-4, August 1966 revised June 1971.

(*5*) RUGGERA, P. S. and R. L. ELDER. Electromagnetic radiation interference with cardiac pacemakers, BRH/DEP 71-5. U.S. Department of Health, Education, and Welfare, Rockville, Md. 20852 (1971).

(*6*) FEDERAL AVIATION ADMINISTRATION. Recommended radiation safety precautions for airborne weather radars, AC No. 20-68. Federal Aviation Administration Advisory Circular (March 11, 1970).